AJNR

# MR Angiography with Three-Dimensional Time-of-Flight and Targeted Maximum-Intensity-Projection Reconstructions in the Follow-up of Intracranial Aneurysms Embolized with Guglielmi Detachable Coils

Veikko J. Kähärä, Seppo K. Seppänen, Pertti S. Ryymin, Pentti Mattila, Timo Kuurne and Erkki M. Laasonen

*AJNR Am J Neuroradiol* 1999, 20 (8) 1470-1475
http://www.ajnr.org/content/20/8/1470

*AJNR Am J Neuroradiol* 20:1470–1475, September 1999

# MR Angiography with Three-Dimensional Time-of-Flight and Targeted Maximum-Intensity-Projection Reconstructions in the Follow-up of Intracranial Aneurysms Embolized with Guglielmi Detachable Coils

Veikko J. Kähärä, Seppo K. Seppänen, Pertti S. Ryymin, Pentti Mattila, Timo Kuurne, and Erkki M. Laasonen

***BACKGROUND AND PURPOSE:*** **Intra-arterial contrast angiographies are generally used to confirm treatment results of endovascular neurointerventions such as aneurysm obliteration. We compared MR angiography with digital subtraction angiography (DSA) as a follow-up technique for the detection of aneurysmal remnant cavities and arterial patency in patients treated for intracranial aneurysms with Guglielmi detachable coils (GDCs).**

***METHODS:*** **In 20 consecutive patients, follow-up MR angiography and routine intra-arterial cerebral angiography were performed on the same day 1 to 7 months (mean, 4.5 months) after embolization with GDCs. MR angiographic data were postprocessed for subvolume maximum intensity projections centered on the region of the treated aneurysm. Hard copies of both imaging studies were interpreted independently in a blinded fashion to record and compare remnant cavities, location of residual flow, and adjacent arterial narrowing, using DSA as the standard of reference. The interpreters also established an occlusion grade for the treated aneurysms as evidenced on DSA images and evaluated MR angiograms for artifactual effects.**

***RESULTS:*** **Overall sensitivity and positive predictive value of MR angiography in revealing aneurysmal remnant cavities were both 90%. Specificity in ruling out a remnant cavity with MR angiography was 91%. One remnant cavity was missed by MR angiography, and in five patients, false adjacent arterial encroachments were reported.**

***CONCLUSION:*** **MR angiography may be useful in the long-term follow-up of successfully treated small and medium-sized aneurysms after concurrent primary verification of their occlusion with DSA.**

Intracranial aneurysms are increasingly being treated by endovascular techniques. The number of centers in which Guglielmi detachable coils (GDCs, Target Therapeutics, Fremont, CA) are used to achieve aneurysmal occlusion is constantly increasing, as is the number of patients admitted for repeat digital subtraction angiography (DSA). Because of the relative novelty of this method, the appropriate duration of angiographic follow-up after successful coiling has not yet been determined. Clearly, there is great demand for a noninvasive, rapid, and practical imaging technique for follow-up. Although the capability of MR angiography in screening for untreated aneurysms is fairly well documented (1–3), only a few studies have evaluated its performance relative to contemporary DSA (4, 5). In terms of safety and image quality, MR angiography has been found to be compatible with the presence of GDCs (6). In this blinded prospective study, the sensitivity of MR angiography in the detection of residual flow in remnant cavities and in the evaluation of adjacent artery patency was compared with conventional DSA in the follow-up of 20 consecutive patients who underwent GDC embolization for treatment of intracranial saccular aneurysms. The rate of occurrence of artifactual effects unfavorable to diagnostic accuracy was also evaluated.

Received November 16, 1998; accepted after revision March 13, 1999.

From the Departments of Radiology (V.J.K., S.K.S., P.S.R., P.M., E.M.L.) and Neurosurgery (T.K.), Tampere University Hospital, Finland.

Address reprint requests to Veikko J. Kähärä, Department of Radiology, Tampere University Hospital, P.O. Box 2000, FIN-33521 Tampere, Finland.



## Methods

From December 1997 through June 1998, 20 consecutive patients (11 men and nine women, 22 to 65 years old; mean age, 49 years) with 21 treated aneurysms were admitted to

**TABLE 1: Patient data and aneurysmal characteristics for 20 patients (21 aneurysms) followed up with DSA and MR angiography**

| Case | Age (y)/Sex | SAH | Location (Size, mm) of Aneurysm | | Size (mm) of Remnant Cavity at DSA/MR Angiography | Percentage (%) of Adjacent Artery Stenosis |
|---|---|---|---|---|---|---|
| 1 | 46/M | Yes | R MCA bifurcation | (4) | –/2 (FP) | … |
| 2 | 43/M | Yes | L ACA | (7) | … | B/50 (FP) |
| 3 | 57/F | Yes | R PICA | (3) | … | P/50 (FP) |
| 4 | 42/M | Yes | L ICA | (8) | 2/3 | … |
| 5 | 60/M | Yes | L MCA bifurcation | (4) | … | … |
| 6 | 48/F | No | R ICA | (30) | 15/18 | … |
| 7 | 32/M | Yes | BA | (6) | … | … |
| | | | BA | (2) | … | … |
| 8 | 41/M | No | L MCA trunk | (3) | … | … |
| 9 | 47/F | No | R ACA | (3) | … | B/100 (FP) |
| 10 | 52/M | Yes | L MCA bifurcation | (7) | 3/3 | … |
| 11 | 65/F | Yes | BT | (5) | … | … |
| 12 | 63/M | No | L MCA bifurcation | (12) | 6/6 | … |
| 13 | 55/M | Yes | L SCA | (6) | 2/2 | … |
| 14 | 51/F | Yes | L ICA | (9) | … | … |
| 15 | 58/F | Yes | L ICA | (26) | 7/10 | P/70 (TP) |
| 16 | 54/F | No | L ICA | (5) | … | … |
| 17 | 22/F | No | R ICA | (6) | 2/2 | … |
| 18 | 40/M | Yes | R AcoA | (16) | 5/– (FN) | B/50 (FP) |
| 19 | 50/M | Yes | L ICA | (4) | 3/2 | … |
| 20 | 52/F | Yes | L ACA | (5) | 3/2 | B/100 (FP) |

Note.—ACA indicates anterior cerebral artery; AcoA, anterior communicating artery: BA, basilar artery: BT, basilar tip; ICA, internal cerebral artery; MCA, middle cerebral artery; PICA, posterior inferior cerebellar artery; SCA, superior cerebellar artery; SAH, subarachnoid haemorrhage; FN, false negative; FP, false positive; TP, true positive; B, branch artery; P, parent artery.

our institution for follow-up DSA. On the same day, they were each also examined by MR angiography before the DSA study. The interval between the last embolization and the follow-up studies ranged from 1 to 7 months (mean, 4.5 months).

All 20 patients had been treated endovascularly with GDCs for intracranial saccular aneurysms. In 14 patients, the aneurysms were accompanied by subarachnoid hemorrhage; in the remaining patients, aneurysms were discovered incidentally or because of symptoms caused by their mass effect. Patients were selected for embolotherapy by a neurosurgeon with special regard for clinical status and vascular anatomy. Five aneurysms were located in the posterior circulation; 16 originated from the anterior circulation. The smallest aneurysm, located in the basilar artery, was 2 mm in diameter; two aneurysms were graded as giant in diameter ($>$ 25 mm), two were 11 to 25 mm, and the remaining 16 were 3 to 10 mm in diameter. The aneurysms are characterized in detail in the Table.

All patients were hospitalized solely for DSA follow-up, and all MR angiographic examinations were performed on the same day, before DSA, with the same MR unit. In the standardized study, performed with the head coil, sagittal T1-weighted and axial T2-weighted fast spin-echo (FSE) sequences were obtained. Imaging parameters for the T1-weighted sequence were 400/8/1 (TR/TE/excitations), 24-cm field of view (FOV), 192 $\times$ 256 matrix, and 5-mm section thickness with a 2-mm gap. Parameters for the T2-weighted FSE sequence were 5500/120/3, echo train length of six, 16.5 $\times$ 22-cm FOV, 256 $\times$ 512 matrix, and 5-mm section thickness with a 2-mm gap. For the selected 3D time-of-flight (TOF) MR angiographic sequence, the imaging parameters were 30/3.1/1 with a fractional echo, 30° flip angle, 24 $\times$ 18-cm FOV, 512 $\times$ 256 matrix, and 0.8-mm section thickness. Flow compensation, variable bandwidth, and auto shimming were included. All angiograms were postprocessed off-line on a workstation (Advantage Windows 2.0, GE Medical Systems, Milwaukee, WI). Standard maximum-intensity-projection (MIP) images in 30° increments were generated through the entire imaging volume. The thickness of the subvolumes for targeted MIPs varied from 8 to 30 mm depending on the size of the aneurysm. Postprocessing was performed independently by one team member to ensure the maximum standardized format for the hard-copy presentation and to shield the readers from viewing previous conventional and MR angiograms.

MR angiographic source images, standard and targeted MIP reconstructions, and spin-echo (SE) images were interpreted prospectively in a blinded fashion by two neuroradiologists in consensual fashion without knowledge of the DSA findings. For the MIP images, the maximum dimension of the residual aneurysmal cavity was determined by comparing the size of the cavity with the vessel diameter of the circle of Willis, matched to age and sex, as described by Krabbe-Hartkamp et al (7). Cavities larger than 1 mm in diameter were categorized as remnants. Flow in the remnant cavity was characterized as appearing either in the neck or the body of the aneurysm. The percentage of encroachment of the parent and adjacent distal branch arteries, for any reason, was calculated, and the amount of coil-induced local artifacts was ascertained. On the cross-sectional SE images, the relevant ischemic and other parenchymal lesions were assessed for coiling or primary hemorrhagic events, and the aneurysmal cavities were scrutinized for thrombus formation.

DSA was performed after MR angiography, and routine projections were obtained to locate aneurysmal remnant cavities or encroachment of adjacent arteries. DSA films were regarded as the standard of reference and were interpreted retrospectively and independently, without knowledge of the contemporary MR angiographic studies, by one radiologist with extensive experience in neuroangiography. For the DSA images, the original size of the aneurysm, the size of the remnant cavity

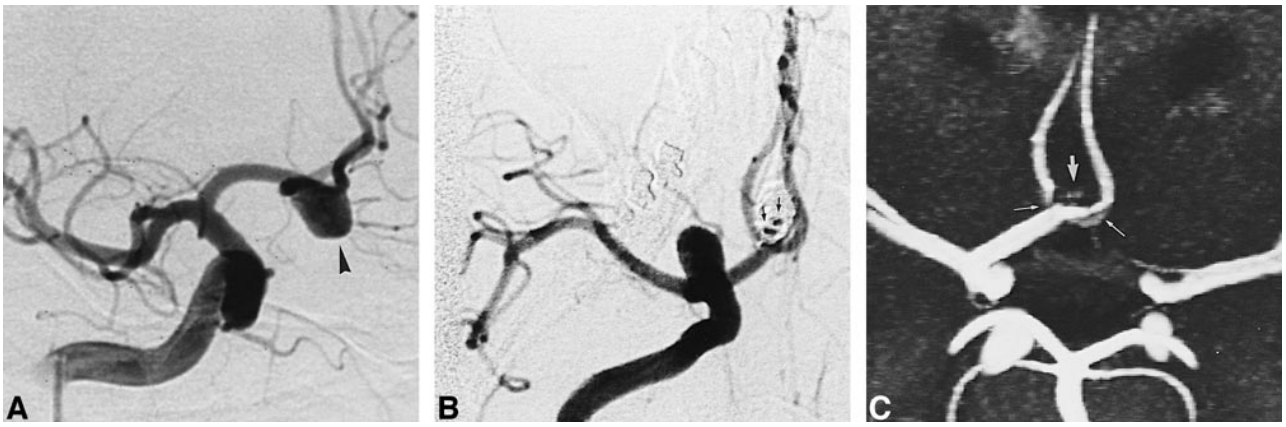


FIG 1. Ruptured aneurysm originating from anterior communicating artery.

*A,* DSA image, oblique projection, right internal carotid injection, shows the aneurysm (*arrowhead*) before embolization.

*B,* DSA image, semiaxial projection, right internal carotid injection 3 months after treatment with electrolytically detachable coils, shows remnant cavity (*arrows*) in the neck area.

*C,* MR angiogram, targeted coronal MIP reconstruction, shows faint signal intensity between the proximal anterior cerebral arteries (*large arrow*), which was not interpreted as an aneurysmal remnant. Note the local encroachment of the anterior cerebral arteries (*small arrows*).

on follow-up studies, the percentage (grade) of achieved occlusion, and the percentage of diameter narrowing in adjacent arteries were evaluated subjectively. When present, the location of residual flow was characterized. Cavities larger than 1 mm in diameter were categorized as remnants.

The study plan was approved by the local ethics committee and informed consent was obtained from the patients.

## Results

Principal results are presented in the Table. All the patients who were admitted for DSA were examined in the MR unit, except for one patient who was claustrophobic. Signal loss due to susceptibility artifacts from nearby clipped aneurysms disqualified one patient from the study; in another patient, the quality of the study deteriorated because of motion artifacts, but the patient was not excluded. One patient with a giant intracavernous internal carotid artery (ICA) aneurysm filled with GDCs experienced a headache and visual disturbance immediately after the examination, but the symptoms abated and the patient was subsequently examined repeatedly in the same MR unit.

### *DSA*

In 13 (62%) of 21 aneurysms, the achieved occlusion grade was judged to be 95% to 100%. Of these, four showed minimal broadening of the neck area, which did not indicate further therapy; in any case, two of these were categorized as remnants, because local luminal dilatation was greater than 1 mm. In the remaining nine aneurysms, further therapy was indicated. Diameters of the remnant cavities ranged from 2 to 15 mm. In the patient with a giant intracavernous ICA aneurysm (case 15), local parent artery encroachment due to coil protrusion was observed. In three patients, other concomitant aneurysms that had been scheduled for further therapy were seen on four-vessel angiograms.

### *MR Imaging and MR Angiography*

Ten remnant cavities were reported, of which nine were true-positives. Diameters of these cavities varied from 2 to 18 mm. There was one false-negative finding, in which MR angiography missed the remnant cavity of an anterior communicating artery aneurysm (Fig 1), and one false-positive finding, in a case of a successfully coiled middle cerebral artery bifurcation aneurysm. MR angiography exaggerated the size of true remnant cavities in three cases and underestimated it in two cases. In 14 cases, there was full agreement between the reviewers as to the postprocedural status of the treated aneurysms. The overall true-positive sensitivity of MR angiography for the detection of remnant cavities was 90%, with a positive predictive value of 90%. In 11 treated aneurysms, categorized as having no remnant cavity on DSA images, MR angiographic findings were in agreement in 10 cases, yielding 91% specificity and negative predictive value.

MR angiography detected one parent artery encroachment seen on DSA images; but in five patients, false arterial encroachment was reported. In one patient, it was the parent artery and in four patients it was the distal branch arteries that seemed affected; of these, the distal branches of the anterior cerebral artery were judged to be totally occluded in two cases. In these five patients, coil artifacts were also reported. Altogether, susceptibility artifacts were reported in six patients. The untreated concomitant aneurysms were detected with MR angiography. Relevant findings on cross-sectional images included gliotic changes as the sequela of in-

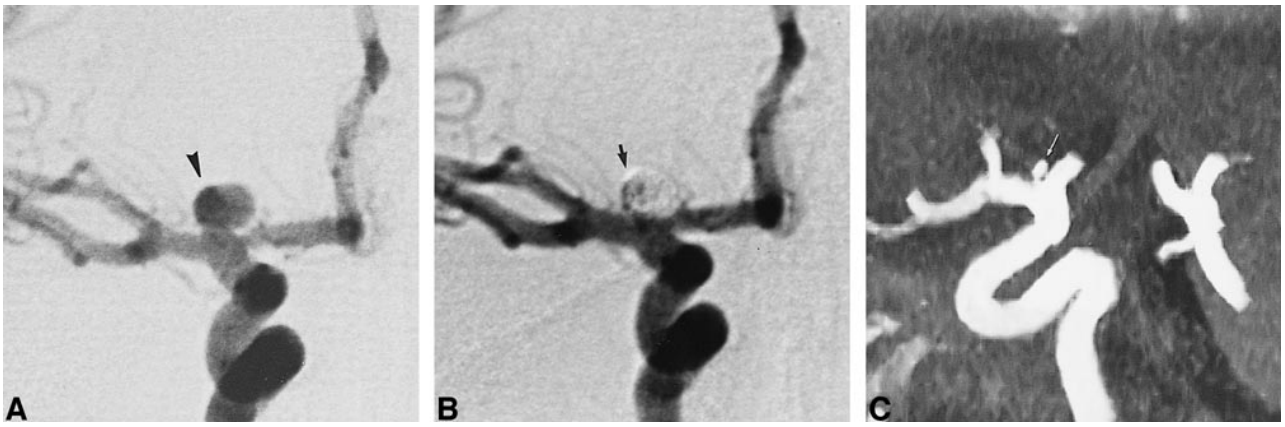


FIG 2. Unruptured aneurysm of the right carotid termination.
*A,* DSA image, anterior projection, right internal carotid injection, shows the aneurysm (*arrowhead*) before embolization.
*B,* Four months after treatment, the aneurysm is subtotally packed with electrolytically detachable coils. The remnant cavity (*arrow*) is faintly seen through the subtracted coil mass.
*C,* MR angiogram, targeted parasagittal MIP reconstruction, clearly shows the remnant cavity (*arrow*).

tracerebral hemorrhage in two cases and of infarction in three cases, of which two were in the vascular territories of the treated aneurysms and one was hydrocephalus.

## Discussion

The main objective of embolotherapy for intracranial aneurysms is to prevent bleeding. All remnants should be regarded as potential bleeders, although an occlusion grade approaching 100% with slight vessel dilatation in the neck area is generally regarded as angiographically sufficient. Often in such cases, safe obliteration of the remnant with GDCs might prove impossible. In any event, the value of a follow-up technique depends on its ability to detect a remnant cavity. There is good reason to regard DSA as the standard of reference, and, as our series reveals, 3D-TOF MR angiography does not match this technique's sensitivity, although, in individual cases, MR angiography may demonstrate a remnant cavity quite convincingly as compared with DSA (Fig 2).

Brugiéres et al (8) and Huston et al (9) have reported the 3D-TOF technique to be inferior to 3D phase-contrast imaging in demonstrating slow flow in large untreated aneurysms ($>$ 15 mm) because of saturation effects, although Araki et al (10) described the pitfalls of 3D phase-contrast imaging in detecting unruptured aneurysms as compared with 3D-TOF MR angiography. Recently, Atlas et al (2) concluded that in screening studies, 3D-TOF imaging barely detects very small aneurysms ($<$ 3 mm) and characterizes aneurysmal morphology poorly. These authors used advanced postprocessing (STANDOUT) techniques, and achieved a mean sensitivity of 75% in the detection of untreated aneurysms. The importance of aneurysmal size was underscored earlier by Huston et al (11), who regarded 5 mm as the critical diameter for achieving sensitivity in applying both the 3D-TOF and phase-contrast MR angiographic techniques in screening for untreated aneurysms. The reported overall sensitivity of the 3D-TOF technique was slightly better than that of the phase-contrast technique (56% versus 44%).

Preliminary experience has shown the potential of 3D-TOF MR angiography after GDC embolization. Derdeyn et al (5) reported 100% sensitivity in detecting residual necks using this technique, with few coil-induced artifacts; however, in their study, MR angiographic interpretations were performed with knowledge of the pretreatment DSA findings. In any case, a very small remnant cavity evidently will restrict the sensitivity of MR angiography. The unexpected inherent complexity of flow dynamics previously reported in the imaging of untreated aneurysms will be further complicated by the coil material, although artifactual signal loss induced by the coils may be alleviated by shortening the TE (12). Source images may help in visualizing low-signal-intensity vessels.

MR angiography showed false arterial encroachment in five patients in our series, but there were no correlating parenchymal ischemic lesions on the concurrent cross-sectional SE images. The false impression of arterial narrowing seen on the MIP images cannot be regarded as a serious failure in the potential of MR angiography to identify the remnant cavity, considering the technique's usefulness as a tool for follow-up. In addition to their ability to reveal parenchymal infarctions, supplementary SE images are recommended for their capacity to help detect other habitual complications of subarachnoid hemorrhage, such as hydrocephalus, sequela of intracerebral hemorrhage, and so on. The SE images may also show thrombotic material in the remnant cavity, which might have implications for further therapy. The section thickness we used, however, seriously limits the detection of small thrombi. On the other


FIG 3. Giant unruptured aneurysm originating from the bifurcation of the right ophthalmic artery.

*A,* DSA image, oblique projection, right internal carotid injection 4 months after treatment, shows the aneurysm is subtotally packed with electrolytically detachable coils. A remnant cavity (*arrowheads*) is seen in the neck area.

*B,* MR angiogram, targeted coronal MIP reconstruction, shows scattered high signal intensity in the upper part of the aneurysm (*small arrows*) in addition to the remnant cavity flow (*large arrow*) in the neck area.

*C,* T1-weighted MR image, sagittal view, shows high signal intensity in the upper part of the coiled aneurysm (*arrows*), which does not represent flow but T1 shortening caused by thrombosis between the coil material.

hand, the T1 shortening due to thrombus seen on 3D-TOF MR angiograms may be interpreted as aneurysms. We encountered this phenomenon in one giant aneurysm of the ICA originating from the bifurcation of the ophthalmic artery. On the MR angiogram, it looked as if the flow were within the coil interstices in the dome of the filled aneurysm (Fig 3). The artifactual high-signal rim seen on the border of the other giant aneurysm was not judged erroneously.

Considering the limitations of MR angiography, follow-up of GDC-treated aneurysms can hardly be executed solely by this technique. Nevertheless, for several GDC-packed aneurysms categorized as small or medium-sized (2 to 15 mm), the follow-up MR imaging and 3D-TOF MR angiographic studies, including targeted MIP reconstructions, showed good correlation with DSA findings. In such cases, the primary follow-up MR angiographic examination, supported by concurrent matching DSA findings, could act as a baseline study. Moreover, the status of treated aneurysms could be monitored with MR angiography, sparing these patients further invasive catheter angiographies. Note, however, that these suppositions are supported by subjective estimates of aneurysmal size. One should also be aware of frequent pseudoencroachments of adjacent arteries on MIP images. The policy of MR angiographic follow-up should include the option of DSA and repeated coiling in cases of recurrent aneurysmal cavities. In these cases, postprocessing with virtual endoscopy might be contributory before performing DSA or further embolization.

## Conclusion

Despite the limitations of this study, we conclude that 3D-TOF MR angiography with postprocessing using targeted MIP reconstructions represents a noninvasive and rapid method for the follow-up of GDC-coiled small and medium-sized saccular intracranial aneurysms. This technique may be sufficient for the long-term monitoring of the stability of coiled aneurysms, provided that the achieved intraluminal occlusion shown on the initial MR angiographic follow-up examination is complemented by concurrent DSA. A larger sample of embolized aneurysms will need to be evaluated to establish the actual rates of sensitivity and specificity. MR angiography with 3D-TOF is limited in its ability to detect a slow flow pattern in the remnant cavities of giant aneurysms; thrombus formation may mimic flow, and the patency of arteries adjacent to aneurysms is frequently misrepresented owing to coil-induced artifacts.

## References

1. Schuierer G, Huk WJ, Laub G. **Magnetic resonance angiography of intracranial aneurysms: comparison with intra-arterial digital subtraction angiography.** *Neuroradiology* 1992;35:50–54
2. Atlas SW, Sheppard L, Goldberg HI, Hurst RW, Listerud J, Flamm E. **Intracranial aneurysms: detection and characterization with MR angiography with use of an advanced postprocessing technique in a blinded-reader study.** *Radiology* 1997;203:807–814
3. Ronkainen A, Puranen MI, Hernesniemi JA, et al. **Intracranial aneurysms: MR angiography screening in 400 asymptomatic individuals with increased familial risk.** *Radiology* 1995;195:35–40
4. Cotroneo E, Dazzi M, Gigli R, Guidetti G, Cantore GP, Chiapetta F. **Magnetic resonance angiography for evaluation of intracranial aneurysms treated with Guglielmi detachable coils.** *Riv Neuroradiol* 1998;11:19–25
5. Derdeyn CP, Graves VB, Turski PA, Masaryk AM, Strother CM. **MR angiography of saccular aneurysms after treatment with Guglielmi detachable coils: preliminary experience.** *AJNR Am J Neuroradiol* 1997;18:279–286
6. Hartman J, Nguyen T, Larsen D, Teitelbaum GP. **MR artifacts, heat production, and ferromagnetism of Guglielmi detachable coils.** *AJNR Am J Neuroradiol* 1996;18:497–501
7. Krabbe-Hartkamp MI, van der Grond J, de Leeuw FE, et al. **Circle of Willis: morphologic variation on three-dimensional time-of-flight MR angiograms.** *Radiology* 1998;207:103–111

8. Brugiéres P, Blustajn J, Le Guérinel C, Méder JF, Thomas P, Gaston A. **Magnetic resonance angiography of giant intracranial aneurysms.** *Neuroradiology* 1998;40:96–102
9. Huston J III, Nichols DA, Leutmer PH, et al. **Blinded prospective evaluation of sensitivity of MR angiography to known intracranial aneurysms: importance of aneurysm size.** *AJNR Am J Neuroradiol* 1994;15:1607–1614
10. Araki Y, Kohmura E, Tsukaguchi I. **A pitfall in detection of intracranial unruptured aneurysms on three-dimensional phase-contrast MR angiography.** *AJNR Am J Neuroradiol* 1994;15: 1618–1623
11. Huston J III, Rufenacht DA, Ehman RL, Wiebers DO. **Intracranial aneurysms and vascular malformations: comparison of time of flight and phase contrast MR angiography.** *Radiology* 1991;181:721–730
12. Gönner F, Heid O, Remonda L, et al. **MR angiography with ultrashort echo time in cerebral aneurysms treated with Guglielmi detachable coils.** *AJNR Am J Neuroradiol* 1998;19:1324–1328